



Research on Plane-Space Algorithm of Binocular Stereo Vision Under Zoom Condition

Xuefei Li¹, Xiaohua Zhang², Qing Shi¹, Huiyu Zhu¹, and Shubin Wang¹ (✉)

¹ College of Electronic Information Engineering, Inner Mongolia University, Hohhot, China
wangshubin@imu.edu.cn

² Department of Foreign Languages, Guizhou University of Commerce, Guiyang, China

Abstract. In the paper, a zoom-plane-space algorithm based on binocular stereo vision is presented to expand the range of the plane-space algorithm. On the basis of the plane-space algorithm, a mathematical model of the zoom-plane-space algorithm is established by introducing the zoom function. According to the optical imaging principle, the imaging model of the zoom image sensor is established and the input point coordinates of the left image sensor without zoom are calculated with this model. Finally, the position coordinates of the target point can be obtained by bringing the converted input point coordinates into the plane-space algorithm. The algorithm is simulated by using the Matplotlib library based on Python3.6. The simulation data show that the error of the algorithm is about 0.04 m when the horizontal coordinates of the target point are moved in steps of 0.1 for 100 steps.

Keywords: Binocular stereo vision · Optical zoom · Zoom-plane-space algorithm

1 Introduction

In the future development of automobile and transportation technology, Internet of vehicles (IoV) technology is regarded as the main technical means to solve the existing traffic problems. In the IoV application scenarios, a multi-sensor fusion network is used to detect information about the surrounding environment, in which the visual sensors are mainly responsible for obstacle detection and distance measurement. Binocular stereo vision (BSV) technology can effectively obtain the distance information in three-dimensional spatial scene. The advantages like high efficiency, suitable accuracy and simple system structure make it very applicable in such fields as unmanned driving and target tracking [1–4].

The main task of BSV algorithm is to obtain the coordinate information of the target object by calculating the position deviation between the corresponding points of images, according to which target matching is an important step in BSV ranging algorithms, therefore many scholars have improved the performance of BSV algorithms by enhancing the accuracy of target matching in binocular ranging algorithms [5–7]. The

BSV ranging algorithm determines the mapping relationship between the target point in the world coordinate system and the pixel coordinate system through the camera stereo calibration. Hence, some researchers also improve the solution accuracy of 3D world coordinate by improving the accuracy of binocular vision calibration [8–10]. Similarly, based on the parallax principle and the structural characteristics of the elements of image sensor, Enshuo Zhang et al. of our research group established the similarity transformation model, and proposed the plane-space algorithm, which can calculate the three-dimensional coordinates of the target point according to the binocular imaging position, and this calculation is high in precision and simple in algorithm structure [11]. However, most current stereo vision systems, including the plane-space algorithm, are mainly fixed focus stereo vision systems. Considering the scene range, in the IoV application environment, the field of view and image resolution of the fixed focus camera are very limited. Compared with the traditional fixed focus stereo vision system, the zoom stereo vision system has obvious advantages, i.e., it can obtain more and farther traffic scene information. The detection, recognition and tracking of the target objects with different depths in the traffic scene can be achieved in different scenes by adjusting the focal length of the camera.

In the environment of IoV, the maximum range of object detection of driverless vehicles limits the maximum speed of the vehicle. Therefore, based on the plane-space algorithm proposed by our project team, the paper aims to solve the problem that the traditional fixed focus stereo vision system cannot warn the collision of high-speed vehicles due to the short measurement distance, and proposes a zoom-plane-space algorithm based on BSV, which can effectively expand the range of the algorithm and play a positive role in vehicle collision warning and improving road traffic safety, etc.

2 Zoom-Plane-Space Algorithm

2.1 Algorithm Model

Figure 1 is the zoom-plane-space algorithm model, where rectangles $A_{1_1}A_{1_2}A_{1_3}A_{1_4}$, $A_{2_1}A_{2_2}A_{2_3}A_{2_4}$ are the positions and sizes of the photosensitive element when the focal lengths of the left and right image sensors of the binocular ranging system are the same, and rectangle $A_{3_1}A_{3_2}A_{3_3}A_{3_4}$ are the positions and sizes of the photosensitive element of the left image sensor after zooming. The plane-space algorithm model is composed of $A_{1_1}A_{1_2}A_{1_3}A_{1_4}$ and $A_{2_1}A_{2_2}A_{2_3}A_{2_4}$, while in the zoom-plane-space algorithm model, an additional $A_{3_1}A_{3_2}A_{3_3}A_{3_4}$ overlaps with $A_{1_1}A_{1_2}A_{1_3}A_{1_4}$, therefore the two rectangles are drawn as shown in Fig. 1 for convenience of observation. Point E is the measured target, and points E_1 , E_2 and E_3 are the projections of point E on image sensors $A_{1_1}A_{1_2}A_{1_3}A_{1_4}$, $A_{2_1}A_{2_2}A_{2_3}A_{2_4}$ and $A_{3_1}A_{3_2}A_{3_3}A_{3_4}$. X_{o1} , X_{o2} and X_{o3} are the rear focus corresponding to image sensors $A_{1_1}A_{1_2}A_{1_3}A_{1_4}$, $A_{2_1}A_{2_2}A_{2_3}A_{2_4}$ and $A_{3_1}A_{3_2}A_{3_3}A_{3_4}$. X_{o1} and X_{o2} are on the x-axis, and X_{o3} is always on the optical axis of the left image sensor. O_1 , O_2 and O_3 are the projection coordinates of the optical axis corresponding to image sensors $A_{1_1}A_{1_2}A_{1_3}A_{1_4}$, $A_{2_1}A_{2_2}A_{2_3}A_{2_4}$ and $A_{3_1}A_{3_2}A_{3_3}A_{3_4}$.

The distance between the left (right) image sensor and the point X_{o1} (X_{o2}) is y_1 , let the coordinates of points $E_1(x_1, y_1, z_1)$, $E_2(x_2, y_1, z_2)$, $E_3(x_3, y_1, z_3)$, $O_1(x_{o1}, y_1, 0)$,

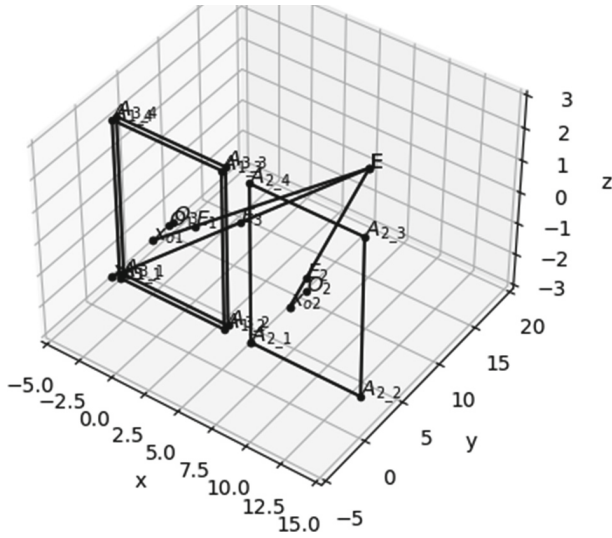


Fig. 1. Zoom-plane-space algorithm model

$O_2(x_{o2}, y_1, 0)$, $O_3(x_{o3}, y_1, 0)$, $x_{o1}(x_{o1}, 0, 0)$, $x_{o2}(x_{o2}, 0, 0)$, $x_{o3}(x_{o1}, -df, 0)$ be known. If the target is calculated according to points $E_1(x_1, y_1, z_1)$ and $E_2(x_2, y_1, z_2)$, the coordinates $E(x, y, z)$ of the target point can be obtained according to the plane space algorithm:

$$\begin{cases} x = \frac{x_1x_{o2} - x_2x_{o1}}{(x_{o2} - x_{o1}) + (x_1 - x_2)} \\ y = \frac{(x_{o2} - x_{o1})y_1}{(x_{o2} - x_{o1}) + (x_1 - x_2)} \\ z = \frac{(x_{o2} - x_{o1})z_2}{(x_{o2} - x_{o1}) + (x_1 - x_2)} \end{cases} \quad (2.1)$$

When the system zooms, the coordinates $E(x, y, z)$ of the target point must be calculated by points $E_2(x_2, y_1, z_2)$ and $E_3(x_3, y_1, z_3)$. Bring:

$$\begin{cases} x_1 = \frac{x_3 - x_{o1}}{k} + x_{o1} \\ z_1 = \frac{z_3}{k} \\ k = \frac{y_1 + df}{y_1} \end{cases} \quad (2.2)$$

into formula (2.1), and the coordinates of the target point $E(x, y, z)$ is obtained.

2.2 Algorithmic Proof

When the system is not zoomed, the algorithm model is the same as the plane-space algorithm in literature [11], so the formula (2.1) can be verified.

For formula (2.2), the model (top view) of the zoom image sensor (left image sensor) is shown in Fig. 2, where $x_{o1}O_1$ and $x_{o3}O_3$ are the optical axes of the left image sensor.

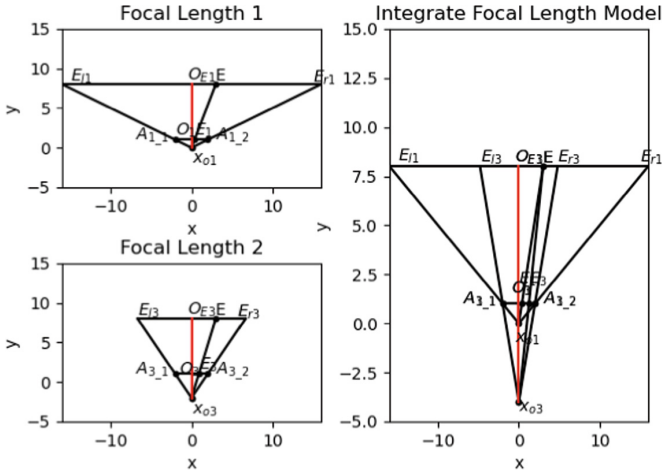


Fig. 2. Imaging model of zoom image sensor (top view)

When the camera zooms to see a targets farther away, it can be derived from the principle of optical imaging:

$$\begin{cases} \frac{O_1E_1}{O_{E_1}E} = \frac{x_{o1}E_1}{x_{o1}E} = \frac{E_1A_{1_2}}{EE_{r1}} \\ O_{E_1}E = O_{E_3}E \\ \frac{O_3E_3}{O_{E_3}E} = \frac{x_{o3}E_3}{x_{o3}E} = \frac{E_3A_{3_2}}{EE_{r3}} \end{cases} \quad (2.3)$$

According to the formula (2.3), it can be deduced that:

$$\frac{O_1E_1/O_3E_3}{O_{E_1}E/O_{E_3}E} = \frac{E_1A_{1_2}/E_3A_{3_2}}{EE_{r1}/EE_{r3}} \quad (2.4)$$

$$\frac{O_1E_1/O_3E_3}{O_{E_1}E/O_{E_3}E} = \frac{x_{o1}E_1/x_{o3}E_3}{x_{o1}E/x_{o3}E} \quad (2.5)$$

And there are:

$$\begin{cases} \frac{x_{o1}E_1}{x_{o1}E} = \frac{x_{o1}O_1}{x_{o1}O_{E_1}} \\ \frac{x_{o3}E_3}{x_{o3}E} = \frac{x_{o3}O_3}{x_{o3}O_{E_3}} \end{cases} \quad (2.6)$$

According to the formula (2.6), the following can be obtained:

$$\frac{x_{o1}E_1/x_{o3}E_3}{x_{o1}E/x_{o3}E} = \frac{x_{o1}O_1/x_{o3}O_3}{x_{o1}O_{E1}/x_{o3}O_{E3}} \quad (2.7)$$

According to the formulas (2.5), (2.7), the following can be deduced:

$$\frac{O_1E_1/O_3E_3}{O_{E1}E/O_{E3}E} = \frac{x_{o1}E_1/x_{o3}E_3}{x_{o1}E/x_{o3}E} = \frac{x_{o1}O_1/x_{o3}O_3}{x_{o1}O_{E1}/x_{o3}O_{E3}} \quad (2.8)$$

That is:

$$\frac{O_1E_1/O_3E_3}{O_{E1}E/O_{E3}E} = \frac{x_{o1}O_1/x_{o3}O_3}{x_{o1}O_{E1}/x_{o3}O_{E3}} \quad (2.9)$$

From Fig. 2:

$$\frac{O_{E1}E}{O_{E3}E} = 1 \quad (2.10)$$

$$x_{o1}O_{E1} - x_{o3}O_{E3} = x_{o1}O_1 - x_{o3}O_3 \quad (2.11)$$

From the formula (2.11), it is deduced that:

$$\frac{x_{o1}O_{E1}}{x_{o3}O_{E3}} = \frac{x_{o3}O_{E3} + x_{o1}O_1 - x_{o3}O_3}{x_{o3}O_{E3}} \quad (2.12)$$

Usually the focal length of the image sensor is in millimeters, while the distance of the target measured is in meters, so it can be obtained:

$$\frac{x_{o1}O_1 - x_{o3}O_3}{x_{o3}O_{E3}} \approx 0 \quad (2.13)$$

According to the formulas (2.12), (2.13), the following can be calculated:

$$\frac{x_{o1}O_{E1}}{x_{o3}O_{E3}} \approx 1 \quad (2.14)$$

By substituting formulas (2.10), (2.14) into formulas (2.9), it can be deduced that:

$$\frac{O_1E_1}{O_3E_3} = \frac{x_{o1}O_1}{x_{o3}O_3} \quad (2.15)$$

Therefore, the following results can be derived:

$$\frac{y_1 + df}{y_1} = \frac{x_3 - x_{o1}}{x_1 - x_{o1}} \quad (2.16)$$

The left view of the imaging model of the zoom image sensor, as shown in Fig. 3. From Fig. 3, a formula (2.15) can also be obtained, and the following results can be derived:

$$\frac{y_1 + df}{y_1} = \frac{z_3}{z_1} \quad (2.17)$$

Therefore, according to the formulas (2.16), (2.17), the formula (2.2) can be proved. To sum up, the algorithm is validated.

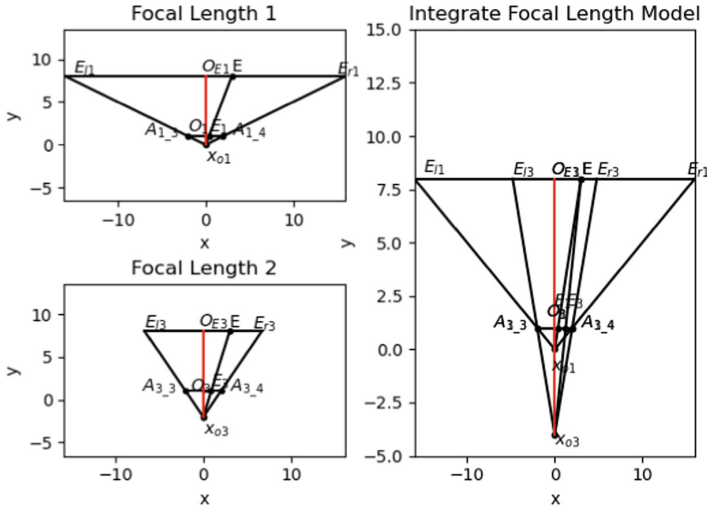


Fig. 3. Imaging model of zoom image sensor (left view)

3 Simulation and Analysis

Based on Matplotlib library of Python3.6, this paper completes all simulation analysis. First, the target point is set and the projected coordinates of the target on the image sensor are calculated according to the principle of optical imaging. Then the input values of the algorithm are determined according to the projected coordinates, and the algorithm values of the target coordinates are calculated by substituting the input values into the algorithm. Finally, the algorithm accuracy is evaluated by comparing the target algorithm values with the set standard values.

3.1 Parameters and Methods of Simulation

The parameters needed for simulation include the pixel width of the image sensor: w , the pixel height of the image sensor: h , the focal length of the left image sensor before or after zooming: f_1 or f_2 , the spacing between left and right image sensors: d , the pixel size: $sizePixel$, the location of the target point: $ObjPont(x, y, z)$ and the number of simulation experiments: Cnt .

The method of calculating model parameters by simulation parameters is as follows:

$$\begin{cases} x_{o1} = \frac{w}{2} \\ x_{o2} = \frac{3}{2}w + d \\ y_1 = 1000 \times \frac{f_1}{sizePixel} \end{cases} \quad (3.1)$$

First, the parameters x_{o1} , x_{o2} and y_1 of the simulation model are calculated according to the formula (3.1). Then a target $ObjPont(x, y, z)$ is set and named the standard value,

and the input values of the plane-space algorithm and the zoom-plane-space algorithm are calculated according to the principle of optical imaging. Next, the target values of the plane-space algorithm and the zoom-plane-space algorithm are calculated according to the parameters obtained, and the values are named as the algorithm values. Finally, the coordinate performance curve is drawn with the algorithm value as the transverse coordinate and the standard value as the vertical coordinate, and the performance of the algorithm is evaluated with the coordinate performance curve. The ideal coordinate performance curve is a straight line with a slope of 1 and an intercept of 0.

3.2 Result Analysis

The initial values of simulation parameters are: $w = 1920$, $h = 1080$, $f_1 = 5$ mm, $f_2 = 10$ mm, $d = 300$ mm, $sizePixel = 6 \mu m$, $ObjPont(50 m, 250 m, 8 m)$, $Cnt = 100$.

When the abscissa of the target point moves laterally by 100 steps in steps of 0.1, the simulation results are shown in Fig. 4. In the figure, the coordinate performance curve of the plane-space algorithm is marked with “singleFocal”, while the coordinate performance curve of the zoom-plane-space algorithm is marked with “multiFocal”.

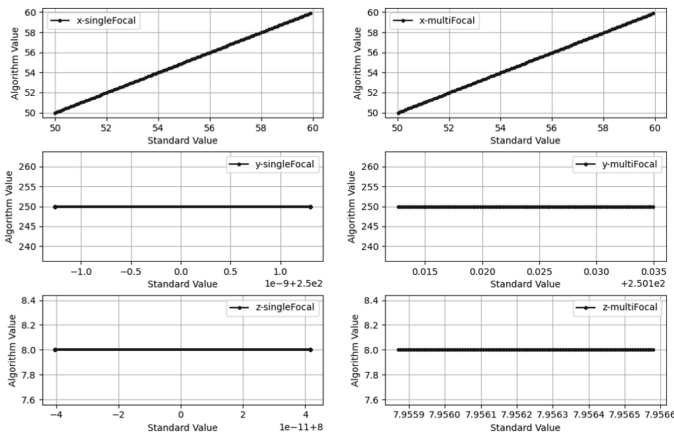


Fig. 4 Simulation image of the target moving along the X-axis

According to Fig. 4, when the measured point moves along the x-axis, the slope of the coordinate performance curve of the x-coordinate is 1, which indicates that the algorithm performs well. When measuring the x-coordinate value of the target point, the zoom-plane-space algorithm and the plane-space algorithm have the same performance. But for y or z values, the error of the algorithm value measured with the plane-space algorithm is between 0–1 m or 0–4 m, while the error of the algorithm value measured with the zoom-plane-space algorithm is about 0.01m or 0.04m.

Therefore, the performance of the zoom-plane-space algorithm is better than that of the plane-space algorithm. In addition, comparing with the plane-space algorithm, when the zoom-plane-space algorithm is used, the measurement range of equipment is relatively larger by adding zoom function, so the comprehensive performance of the

device carrying this algorithm is better than that of the device carrying the plane-space algorithm.

4 Conclusion

Based on the plane-space algorithm, this paper presents a zoom-plane-space algorithm. Using the principle of optical imaging, the algorithm converts the coordinates of the zoomed target point and uses the converted coordinates as input values to the plane-space algorithm. The calculated results are the measured values of the algorithm. The system with the zoom-plane-space algorithm has a larger measurement range than the system with the plane-space algorithm, so the range of the zoom-plane-space algorithm is farther than that of the plane-space algorithm. The simulation data show that the performance of the zoom-plane-space algorithm is better than that of the plane-space algorithm, and the range is larger than that of the plane-space algorithm.

Acknowledgment. Shubin Wang (wangshubin@imu.edu.cn) is the correspondent author and this work was supported by the National Natural Science Foundation of China (61761034), the Natural Science Foundation of Inner Mongolia (2020MS06022).

References

1. Feng, M., Liu, Y., Jiang, P., Wang, J.: Object detection and localization based on binocular vision for autonomous vehicles. *J. Phys: Conf. Ser.* **1544**, 012134 (2020). <https://doi.org/10.1088/1742-6596/1544/1/012134>
2. Fang, L., Guan, Z., Li, J.: Automatic roadblock identification algorithm for unmanned vehicles based on binocular vision. *Wireless Communications and Mobile Computing*, vol. 2021, Article ID 3333754, p. 7, (2021)
3. Xu, Y., Dong, Y., Li, J., Wu, X.: Research on target tracking algorithm based on parallel binocular camera. In: 2019 IEEE 8th Joint International Information Technology and Artificial Intelligence Conference (ITAIC), pp. 1483–1486 (2019)
4. She, H., Yang, X., Shi, Y., Fen, B., Ye, H., Liu, W.: Design and implementation of a target tracking and ranging system based on binocular vision. *IEEE Int. Conf. Recent Adv. Syst. Sci. Eng. (RASSE)* **2021**, 1–5 (2021). <https://doi.org/10.1109/RASSE53195.2021.9686859>
5. Zhang, L., et al.: The SGM Algorithm based on Census Transform for Binocular Stereo Vision. *Int. Conf. Mach. Learn. Knowl. Eng. (MLKE)* **2022**, 50–54 (2022). <https://doi.org/10.1109/MLKE55170.2022.00015>
6. Gai, Q.: Optimization of stereo matching in 3D reconstruction based on binocular vision. *J. Phys. Conf.* **960**(1), 012029 (2018)
7. Y. Wei and Y. Xi, "Optimization of 3-D Pose Measurement Method Based on Binocular Vision," in *IEEE Transactions on Instrumentation and Measurement*, vol. 71, pp. 1–12, 2022, Art no. 8501312, doi: <https://doi.org/10.1109/TIM.2022.3149334>
8. Gao, Z., et al.: Stereo camera calibration for large field of view digital image correlation using zoom lens. *Measurement* **185**, 109999 (2021). ISSN 0263–2241
9. Li, Y.: A calibration method of computer vision system based on dual attention mechanism. *Image Vis. Comput.* **103**, 104039 (2020). ISSN 0262–8856

10. Huang, S., Gu, F., Cheng, Z., Song, Z.: A joint calibration method for the 3D sensing system composed with ToF and stereo camera. *IEEE Int. Conf. Inf. Autom. (ICIA)* **2018**, 905–910 (2018)
11. Zhang, E., Wang, S., Sun, Y.: A new binocular stereovision measurement by using plane-space algorithm. In: Liang, Q., Jiasong, Mu., Jia, M., Wang, W., Feng, X., Zhang, B. (eds.) *Communications, Signal Processing, and Systems: Proceedings of the 2017 International Conference on Communications, Signal Processing, and Systems*, pp. 622–628. Springer Singapore, Singapore (2019). https://doi.org/10.1007/978-981-10-6571-2_76